International Journal on Magnetic Particle Imaging
Vol 8, No 1, Suppl 1, Article ID 2203026, 4 Pages

Infinite Science Publishing

Proceedings Article

High-resolution MPI with spatially resolved measurement on field free lines

Guang Jia[a,*] · Liyu Huang[b] · Ze Wang[a] · Xiaofeng Liang[a] · Yu Zhang[a] · Yifei Zhang[a] · Qiguang Miao[a] · Kai Hu[c] · Tanping Li[c] · Ying Wang[d] · Li Xi[d] · Xin Feng[e] · Hui Hui[e] · Jie Tian[e]

[a]School of Computer Science and Technology, Xidian University, Xi'an Shaanxi 710071, China
[b]School of Biological Science, Xidian University, Xi'an Shaanxi 710071, China
[c]School of Physics, Xidian University, Xi'an, Shaanxi 710071, China
[d]School of Physical Science and Technology, Lanzhou University, Lanzhou, Gansu 730000, China
[e]CAS Key Laboratory of Molecular Imaging, Institute of Automation, Chinese Academy of Sciences, Beijing, 100190, China
*Corresponding author, email: gjia@xidian.edu.cn

Abstract

In magnetic particle imaging (MPI), 1D projected signals can be collected by exciting magnetic particles on a field free line (FFL) with a homogeneous excitation field. The movements and rotations of FFL with projection reconstructions generate 2D and 3D images of magnetic nanoparticles. The image resolution is heavily relying on the wideness of FFL, which is limited by the currently available maximal gradient strength. We proposed an additional gradient field with the same direction as the FFL for pulsed excitation and 1D spatial encoding. The spatial encoding steps include different gradient excitation profiles along with the FFL. System matrix for 1D image reconstruction is based on the relaxation-induced decay signal during the flat portion of pulsed square-wave excitation. For larger magnetic particles, our simulation shows that the pulsed excitation field with a greater flat portion generates a 1D bar phantom image with higher correlation and higher spatial resolution. With parallel FFL movements, high-resolution 2D images of human brain-sized Shepp-Logan phantom and clinical transverse MRA datasets are reconstructed by spatially resolved measurement of magnetic nanoparticles on FFLs.

I. Introduction

In MPI, signal localization is achieved by means of a field free region (FFR) such as field free point (FFP) or field free line (FFL), in which magnetic nanoparticles can be freely excited to contribute signal [1]. It is a big challenge to generate a narrow FFL with clinically usable spatial resolution using currently available hardware [2].

In this paper, we present the high-resolution tomographic imaging method of gradient-based pulsed excitation and relaxation encoding. Linear gradient coils are used to generate an FFL-direction gradient field and to excite magnetic nanoparticles on the FFL. Pulsed square-wave excitation along the FFL direction is implemented to generate relaxation decay signal from nanoparticles [3]. 1D encoding along the FFL direction is carried out by applying different homogeneous excitation field offsets as encoding steps for system matrix-based 1D reconstruction. Parallel movements of FFLs with 1D gradient encoding are simulated to generate 2D high-resolution images.

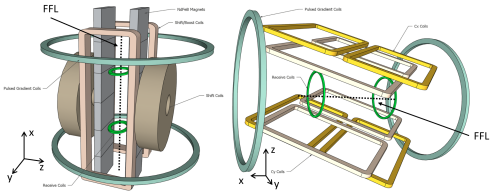

Figure 1: Diagram of two FFL-based MPI systems with pulsed gradient excitation. Left: permanent NdFeB magnets were used to generate a vertical FFL. The vertical movement of the pulsed gradient coils was used for 1D relaxation encoding. Right: open-sided MPI system with electronically rotating FFL. Receiver coils can collect relaxation-induced decay signals from magnetic nanoparticles for high-resolution imaging.

II. Theory

In this section, we describe the theory of gradient field excitation and encoding on an FFL. We use the convention that all excitation field directions are oriented along x axis. All excitation fields have the same frequency without phase difference. We assume there is no residue signal at the end of each pulse cycle that can go into the next pulse cycle, so we don't need to consider steady-state establishment.

II.I. Gradient Excitation Field

First, we borrow x, y, z gradient coils from human-sized clinical MRI scanner with the same shape, size, power supply, and control system for excitation and encoding (Fig. 1). These gradient coils all provide a magnetic field along x direction. However, the fields are linearly varying along the FFL direction:

$$\mathbf{H_G}(\mathbf{r},t) = G_x(t)x\hat{\mathbf{i}} + G_y(t)y\hat{\mathbf{i}} + G_z(t)z\hat{\mathbf{i}}. \quad (1)$$

To excite magnetic particles, the current in gradient coils varies in a pulsed form, such that the gradient amplitude has the pulsed form:

$$G(t) = -G_0 \sum_{n=0}^{N-1} (-1)^n \Pi(2ft - n) \quad (2)$$

where G_0 is the gradient excitation field strength, f is the excitation field frequency, and Π is the rectangular function [3].

II.II. Homogeneous Excitation Field

Second, we need a homogeneous excitation magnetic field. The field direction is also along x axis. By varying the homogeneous excitation magnetic field strength as encoding steps, we can acquire signals from different field distribution profiles for 1D reconstruction.

$$H_A(t) = -A_0 \sum_{n=0}^{N-1} (-1)^n \Pi(2ft - n) \quad (3)$$

where A_0 is the homogeneous excitation field strength.

II.III. Relaxation Decay Signal

The receiver coils can be used to collect the x-direction magnetization changes of magnetic nanoparticles on the FFL. The receiver coils can be any type of radiofrequency receiver coils, such as a full solenoid coil, Helmholtz coil, surface coil, or phased array coils. The receiver coil shape should be designed to efficiently collect the magnetization changes and fit in the scanner and patient bed. The voltage signal induced in the receive coil can be described as

$$u(t) = -\int_{FFL} \mu_0 \left(\frac{d\tilde{M}(x,t)}{dt} * R(t) \right) s(x)c(x)d(x), \quad (4)$$

where μ_0 denotes permeability of free space and $s(x)$ the sensitivity of receive coil. $c(x)$ is the particle concentration on the FFL. $R(t)$ is the Debye relaxation kernel of the nanoparticles:

$$R(t) = \frac{1}{\tau} exp(\frac{-t}{\tau}) S(t). \quad (5)$$

Where $S(t)$ is the Heaviside step function and τ is the relaxation time constant. Without relaxation, the voltage signal is deemed as an adiabatic signal and zero during the flat portion of the pulsed excitation. Relaxation of nanoparticles induces magnetization lag and signal decay during the flat portion (Fig. 2 Left).

This study combines pulsed gradient excitation and FFL-based MPI for high-resolution imaging. As the number of nanoparticles on an FFL is greater than in an FFP, FFL-based MPI scanners exhibit high sensitivity and are suitable for large imaging volumes, such as human in vivo imaging. Our preliminary experiment showed that Synomag-D yielded a two-fold signal amplitude when compared with Perimag. The outcome facilitated the use of Synomag-D for high-resolution images requiring a high signal-to-noise ratio (SNR).

II.IV. 1D FFL Encoding and Reconstruction

Let's assume the simplest case is that 1D straight line phantom along x axis (FFL direction) with the length as the field of view (FOV). The magnetic particle distribution along x axis is $c(x)$. If the expected image resolution is Δx, The 1D encoding step should be $N = FOV/\Delta x + 1$.

For 1D encoding, we set $\theta = 0°$, $\phi = 90°$, such that the gradient and FFL is along x direction, i.e. $G_y = G_z = 0$. The corresponding N excitation profiles are:

$$G_x x + H_{A1}, G_x x + H_{A2}, \ldots, G_x x + H_{AN}. \quad (6)$$

For each step, the decay signal $AUC_{flat,i}$ is

$$AUC_{flat,i} = \sum_{j=1}^{N} AUC_{RX,i}(x_j)c(x_j),\ i = 1,2,\ldots,N. \quad (7)$$

10.18416/ijmpi.2022.2203026

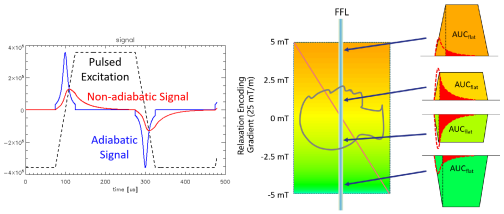

Figure 2: Left: the adiabatic signal was calculated using the Langevin function under pulsed excitation. The non-adiabatic signal was calculated using the Debye relaxation model and was non-zero during the flat portion due to relaxation effects. Right: the relaxation-induced decay signal AUC exhibited a non-linear relationship with the pulsed excitation field amplitude.

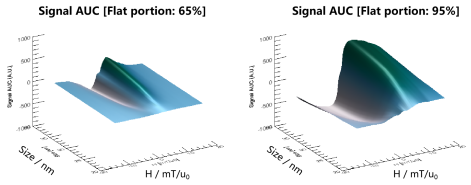

Figure 3: Signal AUC_{flat} vs. pulsed excitation fields with different flat portions (65% and 95%) and particle sizes (20 to 38 nm).

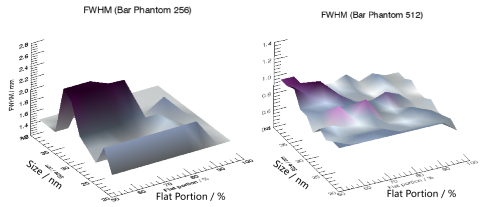

Figure 4: FWHM measurements using 256 and 512 encoding steps. Particles with different sizes and pulsed excitation with different flat portions are used to simulate the scan process and 1D bar phantom reconstruction.

The total decaying signal AUC during flat portion can be calculated from a single particle's AUC_{flat} excited by pulsed gradient field, receiving coil sensitivity and particle concentration at every voxel on the FFL. Based on the nonlinear relationship between decay signal AUC_{flat} and excitation field amplitude, we have N independent linear equations. We can use the matrix to represent these equations as

$$AUC_{RX}C = AUC_{flat}. \tag{8}$$

Where $C = [c(x_1), c(x_2), \dots c(x_N)]$ is the particle concentration vector, $AUC_{flat} = [AUC_{flat,1}, AUC_{flat,2}, \dots, AUC_{flat,N}]$ is the decay signal AUC vector, and

$$AUC_{RX} = \begin{bmatrix} AUC_{RX,1}(x_1) & \cdots & AUC_{RX,1}(x_N) \\ \vdots & \ddots & \vdots \\ AUC_{RX,N}(x_1) & \cdots & AUC_{RX,N}(x_N) \end{bmatrix}$$

is the system matrix. The system matrix is determined by gradient and homogeneous excitation field and receiver coil sensitivity map. Based on the measured decay signal AUC vector and known matrix AUC_{RX}, we can solve these equations and acquire the solutions to C, which is the 1D image vector on FFL.

II.V. FFL Movements for 2D and 3D Scan

During a 2D cross-sectional image scan, the parallel movement of the FFL on the cross-section with respect to the object. The gradient direction is kept the same as the FFL direction. The combination of 1D FFL pixels at different locations can form a 2D image.

III. Simulation Experiments

In this section, we describe the simulation process using a gradient pulsed excitation field for relaxation encoding in FFL-based MPI.

III.I. Magnetic Nanoparticles

We simulate a set of magnetic nanoparticles with the particle size varying from 20 to 38 nm. We adapted the relaxation time measurement under square-wave pulsed excitation from a patent by Conolly et al. [4]. The Langevin function is used to estimate the adiabatic signal, from which non-adiabatic signal is calculated using the Debye relaxation model.

III.II. Pulsed Excitation Fields

In the simulation, we set the pulsed excitation frequency as 2.5 kHz. Each cycle with a duration of 400 µs includes one positive square wave and one negative square wave with the same shape and duration. The flat portion is defined as the percentage of gradient field hold time in the whole excitation period. A set of percentages (50% to 95%) was used to simulate the encoding process and to calculate the relaxation-induced decay signal during hold time. Based on the magnetostimulation and SAR analysis in [3], we fix the gradient as 25 mT/m by assuming the FOV as 0.2 m. We set the homogeneous excitation field amplitude as from -2.5 mT to 2.5 mT. The increase in the homogeneous excitation field per step is 19.6 and 9.8 µT for 256 and 512 encoding steps respectively.

III.III. Phantoms and Quality Assessment

1D bar phantom with FOV of 0.2 m is artificially designed with 256 or 512 pixels. The phantoms include line pairs

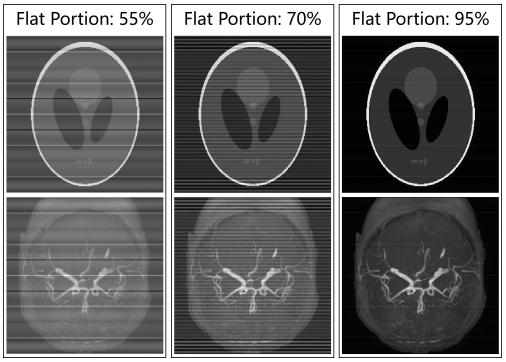

Figure 5: Reconstructed 2D Shepp-Logan phantom and brain MRA projected image using different flat portions in pulsed excitation and particle size of 38 nm.

(lps) with different width (1 to 10 black and white pixels). The full width at half maximum (FWHM) based on the modulation transfer function was calculated to evaluate the resolution of the reconstructed images.

The 2D Shepp-Logan phantom and a total of nine axial brain time-of-flight MRA datasets are included in this study for signal acquisition and reconstruction simulation. The correlation coefficient and root mean square error (RMSE) between the original image and reconstructed image are used for image quality assessment.

IV. Results and Discussions

Relaxation-induced decay signal AUC during flat portion exhibits a non-linear relationship to the pulsed excitation field amplitude. As pulsed excitation field amplitude increases from zero, AUC_{flat} increases due to increasing relaxation time inducing significant lag of the adiabatic signal. AUC_{flat} reaches a peak at 2-7 mTpp and decreases as field amplitude further increases. Peak AUC_{flat} increase with increasing particle size and with the increasing flat portion of pulsed excitation.

The FWHM of the reconstructed 1D bar phantom images became smaller using greater encoding steps. For nanoparticles with a fixed diameter, a greater flat portion enables smaller FWHM with higher spatial resolutions. With 256 and 512 steps, larger nanoparticles and a greater flat portion in pulsed excitation generate 1D bar phantom images with higher resolution.

Reconstructed 2D Shepp-Logan phantom and MRA images show greater correlations and less RMSE using larger-sized nanoparticles and the greater flat portion in puled excitation.

V. Conclusions

We propose 1D spatial encoding on FFL with pulsed gradient excitation fields to solve the spatial resolution problem of current MPI technology. The bio-safe field amplitude and clinical FOV design can overcome the difficulty scaling of hardware and facilitate human in vivo 2D and 3D imaging.

Author's statement

Conflict of interest: Authors state no conflict of interest. Informed consent: Not applicable. Ethical approval: Not applicable.

References

[1] B. Gleich, and J. Weizenecker, "Tomographic imaging using the nonlinear response of magnetic particles," Nature, vol. 435, no. 7046, pp. 1214-7, Jun 30, 2005.

[2] C. B. Top, A. Gungor, S. Ilbey et al., "Trajectory analysis for field free line magnetic particle imaging," Med Phys, vol. 46, no. 4, pp. 1592-1607, Apr, 2019.

[3] Z. W. Tay, D. Hensley, J. Ma et al., "Pulsed Excitation in Magnetic Particle Imaging," IEEE Trans Med Imaging, vol. 38, no. 10, pp. 2389-2399, Oct, 2019.

[4] S. M. Conolly, P. W. Goodwill, D. Hensley et al., Pulsed Magnetic Particle Imaging Systems and Methods, US20190079149, W. I. P. Organization, 2019.

